

Effects Associated with the Thermal Response of the T1 Telephone Transmitter

By C. A. FRITSCH

(Manuscript received April 16, 1968)

The thermal response of the T1 transmitter, when excited by a bias current, is analytically obtained. The thermal expansions which produce a decrease in electrical resistance are described. Good agreement with experimentally measured temperature rises and displacements is demonstrated for the early time transients during which the resistance change occurs. The displacements which produce "thermal packing" are found to be a stronger function of the thermal expansion coefficient of the dome electrode than of any other part of the transmitter assembly.

I. INTRODUCTION

The design of an effective telephone transmitter requires that an acoustic signal (voice) be efficiently converted to an electrical output. One method of performing this function is to use a moving electrode (attached to a diaphragm) as one wall of a chamber containing granular carbon. Thus, if a dc bias current is impressed on the transmitter the resulting variations can be used to operate remote telephone apparatus.

An important factor in the design of such a transmitter is the control of thermal effects, not only caused by variations in ambient conditions but also arising from the heat generated each time the telephone set is connected to the line. These thermal effects result in dimensional changes in the transmitter body, resistance change resulting from temperature rise of the granular carbon itself, and the resistance change caused by thermal expansion of the carbon granules when they are heated by the biasing current. The total effect, which produces a loss of carbon transmitter efficiency, is referred to as "thermal packing."

To assay the relative importance of the various thermal effects it is first useful to ascertain whether the carbon granules should be

treated individually or as a continuum. It has been observed that the contact points resulting from the granule asperities cause a "bunching up" of the current.¹ Consequently, for ac heating in the kilohertz range, the high local rates of heat generation produce larger temperature changes at the points of contact with a proportionately large drop in electrical resistance.¹ However, it can be readily shown (see Appendix A) that the carbon particles are small enough and their thermal diffusivity is high enough so that any local temperature changes are virtually diffused in about one millisecond. Since the resistance changes in the Bell System T1 transmitter* have been observed to take place in about one second,² then the local heating caused by the asperities and the accompanying resistance change can be neglected and the granular carbon can be treated as a continuum.

To determine the effects of thermal expansion in both the microphone body and the granular carbon itself, the temperature distribution throughout the transmitter must be known. Thus, the work reported here consists of a first-approximation type of analysis to determine the temperature distribution in the carbon chamber of the T1 transmitter. The associated thermal effects are then considered with the hope of providing a better insight into what has been experimentally observed.

II. ANALYSIS

2.1 *Thermal Analysis of the Carbon Chamber*

The telephone transmitter design of interest here is shown in Fig. 1. We wish to describe the transient thermal response of this transmitter as the above mentioned dc current is turned on. Geometrically, the carbon chamber consists of a dome (moving) electrode connected with a conical back electrode by a flexible nonconducting chamber closure. If we assume that the surfaces of constant voltage and constant temperature within the carbon aggregate are hemispherical then the walls of the carbon chamber can be considered as two concentric hemispheres (see Fig. 2).

If we also assume for the moment that the relatively heavy back electrode is held at the initial and ambient temperature T_0 , then, the thermal response of carbon and its chamber can be conveniently

* Made by Western Electric Co., the manufacturing and supply unit of the Bell System, and available only to the Bell System.

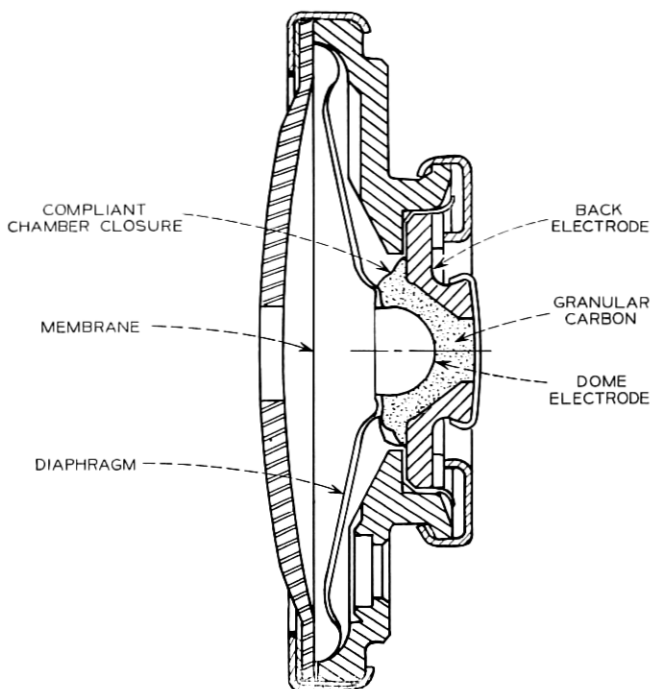


Fig. 1 — Cross section of T1 transmitter.

written in terms of a temperature excess θ defined by

$$\theta = T - T_0. \quad (1)$$

If we further assume that the temperature excursions are small enough so that no significant variations in the physical properties take place then the energy-balance equation is given by

$$\rho c \frac{\partial \theta}{\partial t} = k \nabla^2 \theta + q''', \quad (2)$$

where

k is the effective thermal conductivity of the carbon

ρc is the heat capacity of the carbon

q''' is the rate of heat generation per unit volume.

Because of the angular symmetry of the boundary conditions and the heat generation, gradients in the directions of the angular coordinates can be neglected. Thus, on dividing through by the thermal

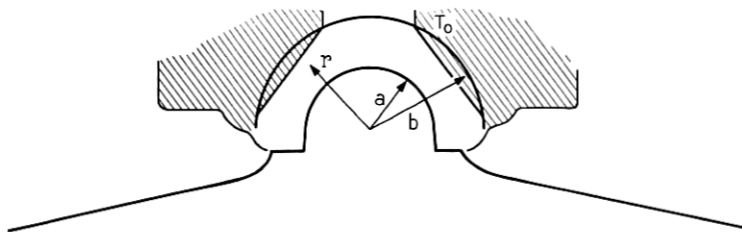


Fig. 2 — Coordinate system for carbon chamber analysis.

conductivity k , equation (2) in spherical coordinates becomes

$$\frac{1}{\kappa} \frac{\partial \theta}{\partial t} = \frac{1}{r^2} \frac{\partial}{\partial r} \left(r^2 \frac{\partial \theta}{\partial r} \right) + \frac{q'''}{k} \quad (3)$$

where κ is the thermal diffusivity.

In general, the heat generation per unit volume is given by the product of the square of the current flow per unit area times the electrical resistivity. Since here we have only radial flow of current I then

$$q'''(r) = (I/2\pi r^2)^2 \rho_e = i_a^2 \rho_e. \quad (4)$$

It can be readily shown that the resistivity ρ_e is related to a total measured resistance R for a cavity formed by two hemispheres of inner radius, a , and outer radius, b , by

$$\rho_e = 2\pi[ab/(b-a)]R. \quad (5)$$

To specify the boundary conditions on our problem we recall that the initial and back electrode temperature are taken to be ambient. To approximate the heat lost by the dome electrode we specify a certain thermal resistance between the dome and some sink at ambient temperature and that resistance is represented by a coefficient h in the so-called "radiation" boundary condition. Consequently, on using (4) and (5) in (3) the following boundary-value problem can be stated.

$$\frac{1}{\kappa} \frac{\partial \theta}{\partial t} = \frac{1}{r^2} \frac{\partial}{\partial r} \left(r^2 \frac{\partial \theta}{\partial r} \right) + \frac{2}{r^4} \left(\frac{ab}{b-a} \right) \beta \quad (6)$$

$$\theta(r, 0) = 0 \quad (7)$$

$$\theta(b, t) = 0 \quad (8)$$

$$k \frac{\partial \theta}{\partial r}(a, t) = h\theta(a, t), \quad (9)$$

where

$$\beta = I^2 R / 4\pi k. \quad (10)$$

The above nonhomogeneous problem in spherical coordinates can be simplified by the following substitutions. If we define the dimensionless variables

$$\tau = \kappa t / (b - a)^2, \quad (11)$$

$$\eta = (b - r) / (b - a), \quad (12)$$

and

$$v(\eta, \tau) = \frac{r\theta(r, t)}{\beta} + \frac{ab}{b - a} (1/r), \quad (13)$$

then the problem specified by (6) through (10) becomes a homogeneous transient conduction problem in a slab with an initial temperature distribution:

$$\frac{\partial v}{\partial \tau} = \frac{\partial^2 v}{\partial \eta^2} \quad (14)$$

$$v(\eta, 0) = F / (1 - F) \left(\frac{1}{1 - (1 - F)\eta} \right) \quad (15)$$

$$v(0, \tau) = F / (1 - F) \quad (16)$$

$$\partial v / \partial \eta (1, \tau) + \frac{(1 - F)}{F} (N_{Bi} + 1) v(1, \tau) = (N_{Bi} + 2) / F, \quad (17)$$

where

$$F = a/b \quad (18a)$$

$$N_{Bi} = ha/k. \quad (18b)$$

N_{Bi} is called the Biot number which characterizes the ratio of the rate at which heat is lost at the dome electrode to the rate at which heat is conducted to it through the granular carbon.

The analytical solution of the transformed problem is relatively straightforward if the dimensionless temperature $v(\eta, \tau)$ is first divided into two functions, one representing the steady-state temperature rise, the other corresponding to the transient response. Thus, we set

$$v(\eta, \tau) = \varphi(\eta) + \vartheta(\eta, \tau). \quad (19)$$

The steady-state portion, $\varphi(\eta)$, satisfies

$$d^2\varphi/d\eta^2 = 0 \quad (20)$$

$$\varphi(0) = F/(1 - F) \quad (21)$$

$$d\varphi/d\eta(1) + \frac{(1 - F)}{F} (N_{Bi} + 1)\varphi(1) = (N_{Bi} + 2)/F. \quad (22)$$

The steady-state solution is then

$$\varphi(\eta) = \left[\frac{2 - F + N_{Bi}(1 - F)}{1 + N_{Bi}(1 - F)} \right] \eta + F/(1 - F). \quad (23)$$

The transient portion of the solution results from letting $\vartheta(\eta, \tau)$ satisfy

$$\partial\vartheta/\partial\tau = \partial^2\vartheta/\partial\eta^2 \quad (24)$$

$$\vartheta(\eta, 0) = F/(1 - F) \left[\frac{1}{1 - (1 - F)\eta} \right] - \varphi(\eta) \quad (25)$$

$$\vartheta(0, \tau) = 0 \quad (26)$$

$$\partial\vartheta/\partial\eta(1, \tau) + \frac{(1 - F)}{F} (N_{Bi} + 1)\vartheta(1, \tau) = 0. \quad (27)$$

The solution to the problem in $\vartheta(\eta, \tau)$ is derived in Appendix B and can be stated as follows:

$$\vartheta(\eta, \tau) = \sum_{n=1}^{\infty} \frac{2(\lambda_n^2 + c_1^2)}{\lambda_n^2 + c_1^2 + c_1} \exp(-\lambda_n^2 \tau) \sin \lambda_n \eta \int_0^1 \vartheta(\eta, 0) \sin \lambda_n \eta d\eta, \quad (28)$$

where λ_n are the positive roots of

$$\lambda_n \cot \lambda_n = -c_1, \quad (29)$$

and the parameter c_1 is defined as

$$c_1 = \frac{(1 - F)}{F} (N_{Bi} + 1). \quad (30)$$

The series solution given above was found to converge too slowly for practical evaluation.* However, the problem specified by (14) through (17) can be readily solved through the use of finite differences. Once $v(\eta, \tau)$ was so determined for various values of N_{Bi} and

* The difficulty resulted from the oscillating nature of the integral in (28). At small values of τ as many as 350 terms were inadequate for convergence.

F , then the temperature rise above ambient $\theta(r,t)$ could be found using (13).

2.2 Temperature Distribution in the Conical Diaphragm

In the analysis of the transient response of the carbon chamber, the boundary condition associated with the dome electrode has specified that the heat loss from every point on the interior surface of the dome electrode is proportional to the difference between the electrode temperature $T(a,t)$ and the ambient temperature T_0 . The constant of proportionality has been designated as h , which is a measure of the impedance of the conical diaphragm to the flow of heat. Thus, the heat flux at the junction between the diaphragm and the dome electrode is given by*

$$q'' = h[T(a, t) - T_0] \cdot \gamma = -k \left. \frac{\partial T}{\partial s} \right|_{s=s_1} \quad (31)$$

where the coordinate system is shown in Fig. 3. The factor γ is defined

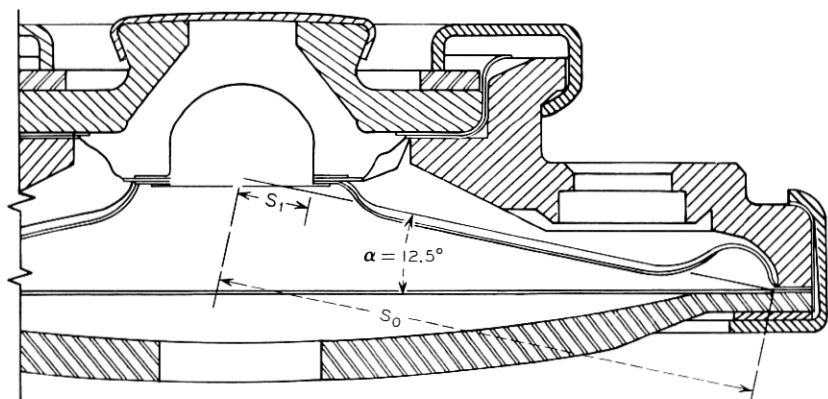


Fig. 3 — Coordinate system for heat flow along the conical diaphragm.

as the ratio of the surface area of the dome to the cross-sectional area of the diaphragm at $s = s_1$. If the thickness of the diaphragm is δ then $\gamma = a/\delta$.

In actuality, the coefficient h as defined by (31) is not a constant since the $\partial T/\partial s|_{s=s_1}$, divided by $[T(a, t) - T_0]$ is still a function of

*It can easily be shown that the heat losses for the dome electrode to the air in contact with it are negligible.

time, somewhat larger at early times than at steady state. This means that the thermal impedance increases from some initial value in proportion to the loss of the capacitive effects as the transient dies out. Thus, the steady-state value of h will be a minimum value.

A more exact approach to the problem would require the simultaneous determination of the transient response of the diaphragm linked to the carbon cavity by a matched heat flux boundary condition. However, if the capacitance of the diaphragm is small compared with the capacitance of the carbon cavity* then the determination of h using the steady-state temperature gradient in (31) should be at least in the correct order of magnitude. Because of the crudeness of other approximations it was felt that the more exact approach was not warranted.

When we perform a heat balance for steady state axially symmetric heat conduction in the conical diaphragm, the following boundary value problem can be stated:

$$d/ds(s \, dT/ds) = 0 \quad (32)$$

$$T(s_1) = T(a, t) \quad (33)$$

$$T(s_0) = T_0. \quad (34)$$

The solution is

$$\frac{T(s) - T(a, t)}{T_0 - T(a, t)} = \frac{\ln(s/s_1)}{\ln(s_0/s_1)}. \quad (35)$$

Differentiating (35) and using the results in (31), we then have for the steady-state approximation

$$h = \frac{\delta k_d \cos 12.5^\circ}{a^2 \ln(s_0/s_1)}, \quad (36)$$

where

$$s_1 = a/\cos 12.5^\circ.$$

2.3 Displacements Resulting from the Thermal Response

To calculate the displacements of the dome electrode we have chosen some rather simplified models for the geometrical configurations and constraints.

First, consider the dome electrode itself. If we assume that the

* The capacitance of the diaphragm is about one tenth the thermal capacitance of the carbon chamber for the T1 transmitter.

edge in contact with the diaphragm is essentially free it can be shown from both physical reasoning and the theory of elasticity that for an unconstrained hemisphere with a uniform temperature change the change in radius is given by

$$\Delta r = \alpha_t \theta(a, t) \cdot a. \quad (37)$$

The calculation of the displacements in the conical diaphragm are somewhat more involved because of the temperature gradient along the diaphragm. We first assume that the cone angle is small enough so that the conical diaphragm can be approximated by a disk. Thus, the displacement in the radial direction is given by³

$$u = (1 + \nu) \frac{\alpha_t}{s} \int_{s_1}^s [T(s) - T_0] s \, ds + C_1 s + C_2/s, \quad (38)$$

where

$T(s)$ is the temperature along the diaphragm as given by (35)

T_0 is the (ambient) temperature in the stress free condition.

If we rewrite (35) in the following form:

$$T(s) - T_0 = [T(a, t) - T_0] \frac{\ln(s/s_0)}{\ln(s_1/s_0)} \quad (39)$$

where $T(a, t) - T_0 = \theta(a, t)$, then (38) becomes

$$u = (1 + \nu) \frac{\alpha_t \theta(a, t)}{\ln(s_1/s_0)} \cdot \left[\frac{s}{2} \ln \left(\frac{s}{s_0} \right) - \frac{s_1^2}{2s} \ln \left(\frac{s_1}{s_0} \right) - \frac{s}{4} + \frac{s_1^2}{4s} \right] + C_1 s + C_2/s. \quad (40)$$

The two constants can be determined from the boundary conditions on the diaphragm. We will assume that the outer edge of the diaphragm is fixed so that

$$u = 0, \quad s = s_0. \quad (41)$$

If we also consider that the inner edge is free so that the radial stress at the location is zero then³

$$du/ds + \nu u/s - (1 + \nu) \alpha_t \theta(a, t) = 0, \quad s = s_1. \quad (42)$$

Applying these conditions to (40) we find that

$$u = (1 + \nu) \frac{\alpha_t \theta(a, t)}{\ln(s_1/s_0)} \left[\frac{s}{2} \ln \left(\frac{s}{s_0} \right) - \frac{s_1^2}{2s} \ln \left(\frac{s_1}{s_0} \right) - \frac{s}{4} + \frac{s_1^2}{4s} \right]$$

$$- \left[s \left(\frac{1-\nu}{1+\nu} \right) + \frac{s_1^2}{s} \right] \left[\frac{\frac{1}{4} - \frac{1}{4} \left(\frac{s_0}{s_1} \right)^2 + \frac{1}{2} \ln \left(\frac{s_0}{s_1} \right)}{1 + \left(\frac{s_0}{s_1} \right)^2 \left(\frac{1-\nu}{1+\nu} \right)} \right]. \quad (43)$$

Since we are primarily interested in the displacement of the dome electrode which is fastened to the diaphragm at $s = s_1$, we first evaluate (43) for that location:

$$u(s_1) = \frac{2s_1\alpha_t\theta(a, t)}{\ln(s_0/s_1)} \left[\frac{\frac{1}{4} - \frac{1}{4} \left(\frac{s_0}{s_1} \right)^2 + \frac{1}{2} \ln \left(\frac{s_0}{s_1} \right)}{1 + \left(\frac{s_0}{s_1} \right)^2 \left(\frac{1-\nu}{1+\nu} \right)} \right]. \quad (44)$$

There are two methods by which the displacement along the slant height of the conical diaphragm can be exhibited as displacement of the dome electrode along the axis of symmetry of the T1 type transmitter. As shown in Fig. 4a, if the diaphragm is rigidly fastened to the dome then the dome displacement resulting from the thermal stresses in the diaphragm are given by

$$\Delta h_{\min} = -u \sin \alpha, \quad (45)$$

so that the axial displacement, Δh , is somewhat less than the displacement along the slant height of the conical diaphragm. Considering the other extreme, as illustrated in Fig. 4b, if the fastening is loose but the dome electrode is rigid then the edge of the diaphragm moves as if up a rigid wall and the axial displacement is amplified

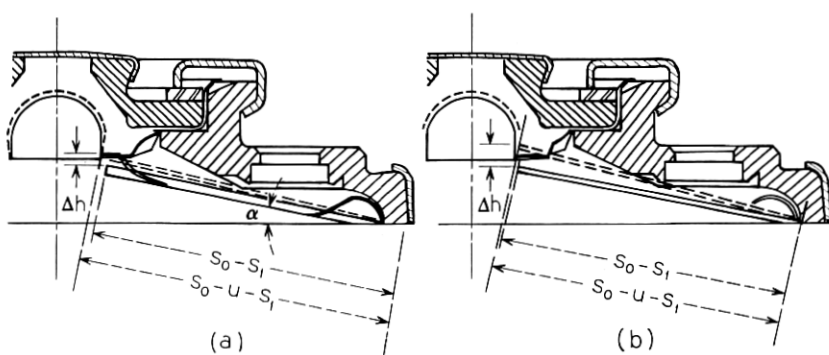


Fig. 4—Displacement of dome electrode resulting from thermal stresses in the diaphragm.

by the sine of the angle. When the growth of the dome electrode, $\alpha_t \theta a$, is taken into account we have

$$\Delta h_{\max} = \frac{\alpha_t \theta a}{\tan \alpha} - \frac{u}{\sin \alpha}. \quad (46)$$

In the actual case the true axial displacement will be somewhere between these two extremes.

III. ANALYTICAL RESULTS

The thermal response of the carbon chamber has been determined for various values of N_{B1} ranging from 0 to 100 and for two values of the shape parameter F . As noted earlier, the conical shaped back electrode has been approximated by a hemisphere of radius b . The choice of the value of b (and hence F) was somewhat arbitrary. Thus, two values were taken for comparison. The character of the approximation is illustrated in Fig. 5. It was felt that the smaller value, $b = 0.44$ cm corresponding to $F = 0.636$, was the better choice.

The results in terms of the temperatures in the slab, $v(\eta, \tau)$, were transformed back to the temperatures in the carbon chamber using (13). Consequently,

$$\frac{\alpha \theta(r, t)}{\beta} = \frac{F}{1 - (1 - F)\eta} [v(\eta, \tau) - v(\eta, 0)]. \quad (47)$$

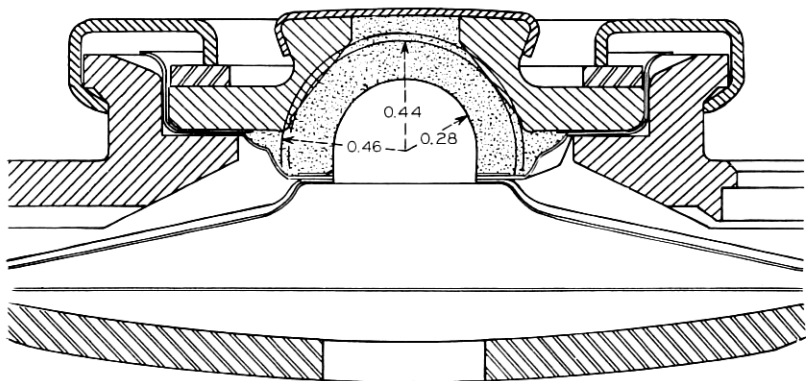


Fig. 5—Approximation of carbon chamber by hemispherical cavity. Indicated radii are in cm.

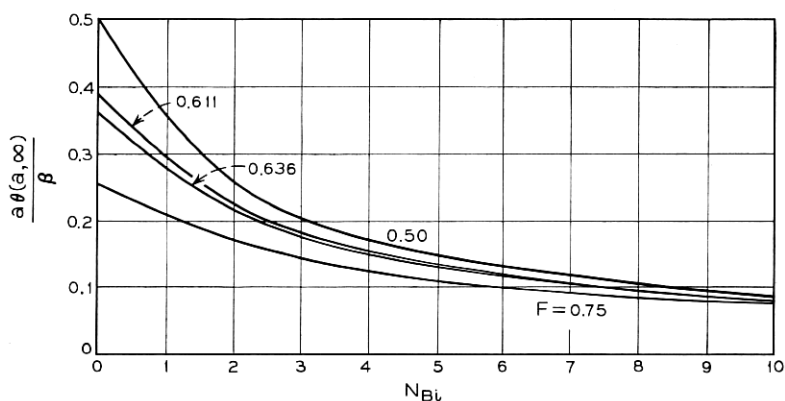


Fig. 6—Dome electrode maximum temperature rise vs N_{Bi} . ($F=0.636$ for standard T1 transmitter.)

Evaluating (47) at $\eta = 1$, the temperature rise of the dome electrode can be expressed as:

$$\frac{a\theta(a, t)}{\beta} = [v(1, \tau) - 1/(1 - F)]. \quad (48)$$

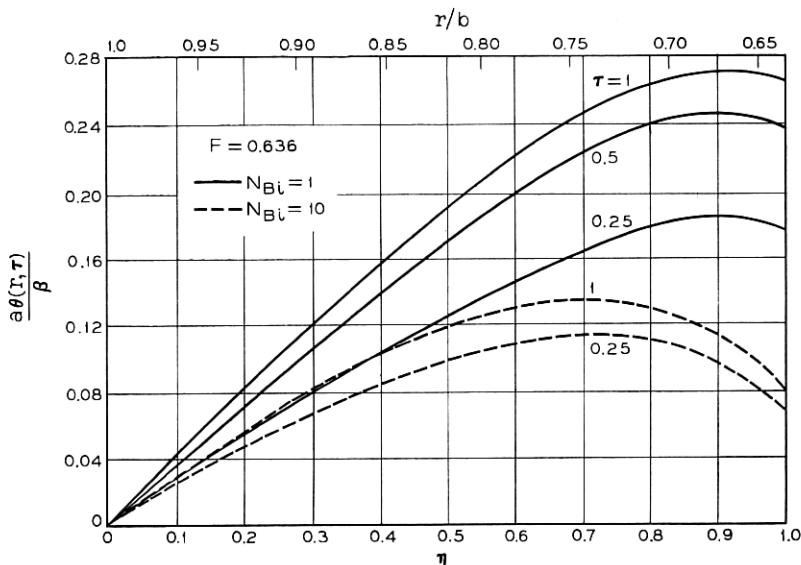


Fig. 7—Temperature distributions at various times for two values of N_{Bi} .

From the steady-state solution (23) the maximum value of $\theta(a,t)$ becomes

$$\frac{a\theta(a, \infty)}{\beta} = \frac{(1 - F)}{1 + (1 - F)N_{Bi}}. \quad (49)$$

This function is plotted in Fig. 6 for various values of F .

The temperature distributions above ambient for $F = 0.636$ and two values of N_{Bi} (1 and 10) are given in Fig. 7 for various times expressed in the nondimensional time variable τ . The value of the abscissa denoted as $\eta = 1$ ($r/b = 0.636$) corresponds to the temperature rise of the dome electrode. As expected, the temperature rise of the dome electrode is substantially decreased as the Biot number is increased. This fact is also demonstrated in Fig. 6.

The "early time" transient response of the T1 transmitter to the "thermal packing" effect will be shown later to be closely linked to the transient temperature changes experienced by the dome electrode. This transient response is illustrated in Fig. 8 as the ratio of $\theta(a,t)/\theta(a, \infty)$ versus τ . The effect of choosing a smaller value of F is also shown for various values of N_{Bi} by the broken lines. It is seen that virtually all of the transient temperature change has taken place by the time that $\tau = 1$. If the thermal time constant τ_o is defined as that value of τ where the transient has decayed to $1/e$ of its value, then the ratio $\theta(a,\tau)/\theta(a, \infty) = 0.632$ at $\tau = \tau_o$. Taking the values of τ_o from Fig. 8 then a curve of τ_o vs N_{Bi} can be drawn for both values of F . These are indicated in Fig. 9 by the notation $\eta = 1$. The thermal time constant for a position which roughly characterizes the maximum temperature within the carbon chamber, that is, $\eta = 0.7$, is also shown.

IV. EXPERIMENTAL OBSERVATIONS AND APPLICATION

Experimental observations have indicated that the electrical resistance of the T1 transmitter is significantly altered when a bias current is imposed. Fischer and Gaudet have attributed the major cause of this change to the thermal expansion of transmitter components resulting from the joulean heating in the carbon.² They tested both the standard T1 transmitter and a similar transmitter with an invar dome, diaphragm, and back electrode. The low expansion coefficient of invar reduced the thermal expansions and hence the invar transmitter packed less than the T1 transmitter. However, the reduction

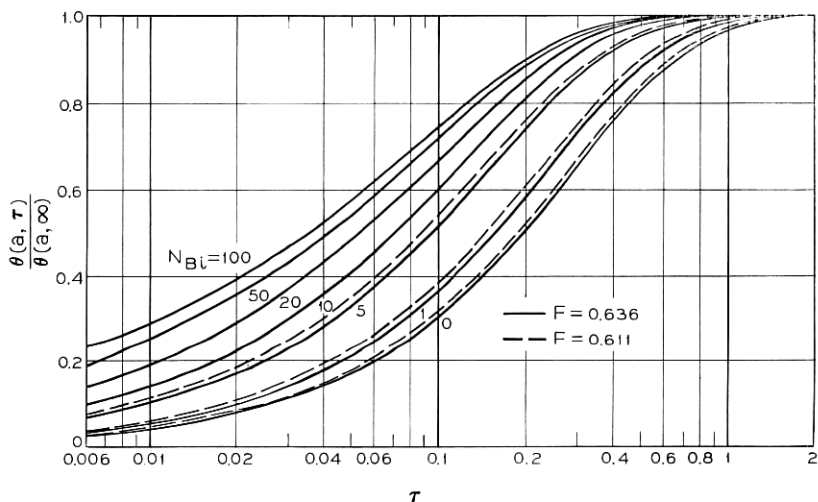


Fig. 8—Transient temperature rise of the dome electrode for various N_{Bi} and two values of F .

was not as significant as had been expected because the thermal resistance of the invar parts was greater and consequently higher temperatures were experienced on the dome electrode.

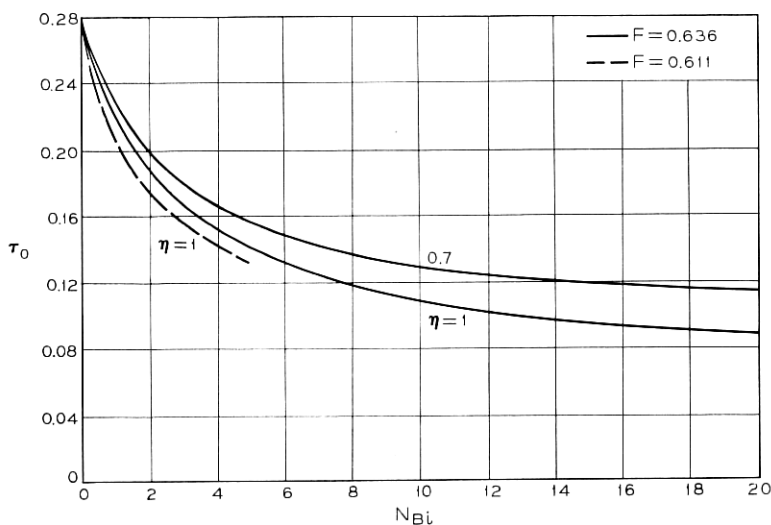


Fig. 9—Thermal time constant at two positions as a function of N_{Bi} .

A detailed description of the thermal effects necessitated measurements of the dome electrode displacement and temperature. These were undertaken by C. Sandahl and P. E. Prettyman. The report has not been published but here is Mr. Sandahl's description of some of the instrumentation.

A flexible silicon semiconductor strain gage, 6 mils square by 50 mils long, was bonded to the diaphragm with epoxy in the region of maximum radial strain. A spherical bead thermistor 5 mils in diameter was attached to the underneath side of the dome electrode at the centerline with pressure sensitive tape.

The strain gage and thermistor were connected into Wheatstone bridge circuits. Bridge excitation was one volt, in order to minimize self-heating of the devices. The thermistor was calibrated in an oil bath using a NBS-calibrated thermometer graduated in 0.01°C . The strain gage was calibrated in deflection of the dome by installing a small front-surface mirror (weight 0.204 gms) on a balsa wood plug in the dome. The transmitter was excited by the JRB circuit (a nearly constant current circuit) at various current levels and the steady-state deflection of the mirror was measured with an optical interferometer. The strain gage bridge output was measured for each increment of deflection.

During each test, thermistor bridge output, strain gage bridge output, JRB circuit voltage across the transmitter, and current through the transmitter were recorded simultaneously on a four-channel Sanborn recorder. Results for four typical tests on a particular transmitter are reproduced in Fig. 10. The test shown in 10d was a repeat of 10c changing only the scale factor on the original recording equipment.

In addition, detailed knowledge of the thermal resistance of granular carbon in a brass container was necessary for the application of the analysis presented here. This thermal resistance was found to consist of two parts: an effective thermal conductivity for a continuum representation of the granular carbon and a thermal contact resistance at the interface between the medium and the container walls. Experimental measurements of these two quantities have been recently completed and are reported in Ref. 4.

In Fig. 10, two types of response are apparent. There is an early time transient for which the back electrode temperature can be assumed constant. After a few seconds the back electrode and the whole transmitter begins to heat up. The subsequent over-all growth coupled with the thermal expansion of the granular carbon itself combines

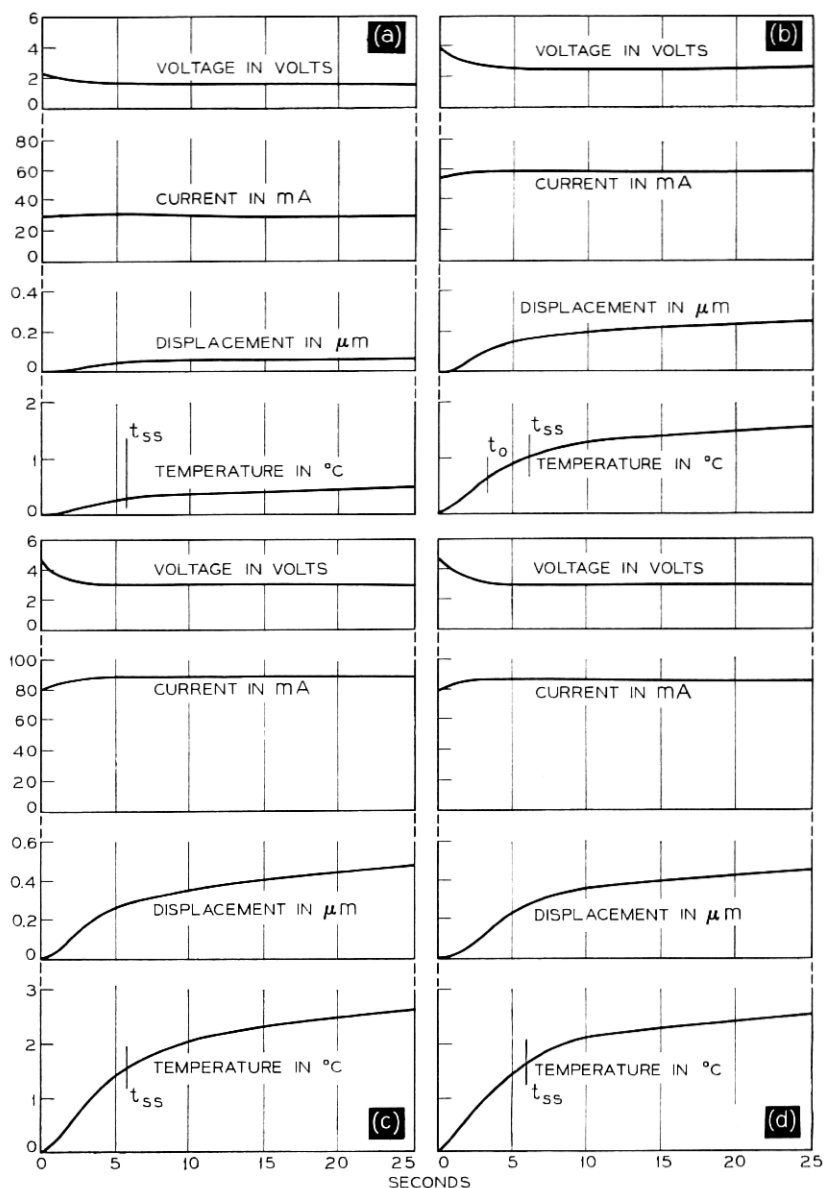


Figure 10. — Transient response of an excited T1 telephone transmitter. (a) Run 1, $\langle IV \rangle_{\text{av transient}} = 0.056W$; (b) run 2, $\langle IV \rangle_{\text{av transient}} = 0.156W$; (c) run 3, $\langle IV \rangle_{\text{av transient}} = 0.264W$; (d) run 4, $\langle IV \rangle_{\text{av transient}} = 0.264W$.

in such a manner that the transmitter resistance (voltage) reaches a constant value. No attempt will be made here to describe analytically this combination of effects at times later than about 6 seconds. However, the early time transient, which produces the resistance change, can be described.

We first calculate N_{Bi} for the standard T1 transmitter. Calculating the thermal conductance of the diaphragm from (36)

$$h = \frac{\delta k_d \cos 12.5^\circ}{a^2 \ln (s_0/s_1)} = 660 \text{ W}/(\text{m}^2 \cdot ^\circ\text{C})$$

when

$$\begin{aligned}\delta &= 0.0076 \text{ cm}, \\ k_d &= 140 \text{ W}/(\text{m} \cdot ^\circ\text{C}), \\ a &= 0.28 \text{ cm}, \\ s_0 &= 2.1 \text{ cm}, \\ s_1 &= 0.286 \text{ cm}.\end{aligned}$$

From Ref. 4 we take the thermal conductivity of the carbon to be 0.24 W per $(\text{m} \cdot ^\circ\text{C})$ and the thermal contact conductance as $h_c = 300$ W per $(\text{m}^2 \cdot ^\circ\text{C})$. Consequently, the total conductance is the sum of the contact conductance in parallel with the conductance of the diaphragm:

$$1/h_{\text{tot}} = 1/660 + 1/300;$$

hence,

$$h_{\text{tot}} = 206 \text{ W}/(\text{m}^2 \cdot ^\circ\text{C}).$$

Using h_{tot} in N_{Bi} we have

$$N_{Bi} = ha/k = 2.4.$$

Turning to Fig. 6 we see that $a\theta(a, \infty)/\beta = 0.19$ and Fig. 9 gives $\tau_o = 0.18$ for this value of N_{Bi} . Now, the thermal diffusivity $\kappa = k/\rho c = 0.32 \times 10^{-6}$ m^2 per second for granular carbon where $\rho = 900$ kg per m^3 and $c = 840$ J per $(\text{kg} \cdot ^\circ\text{C})$ (for the loose state). Consequently,

$$t_0 = \frac{\tau_o(b-a)^2}{\kappa} = 1.4 \text{ seconds},$$

where $b = 0.44$ cm from Fig. 5. In the determination of β we use the average values $\langle IV \rangle_{\text{av}}$ as obtained by a graphical integration of the transient portions of the appropriate curves of Fig. 10. Taking the

value from Fig. 10b as typical we have

$$\beta = \frac{\langle IV \rangle_{av}}{4\pi k} = 5.17 \text{ cm}^\circ\text{C}.$$

Therefore, $\theta = 0.19\beta/a = 3.5^\circ\text{C}$.

By comparing the time constant of 1.4 seconds to the measured values of t_o in the range of 3 seconds, one could say that this is reasonable agreement especially since the capacitance effects of the diaphragm and the electrodes have been neglected in the analysis. The capacitance in the real situation would tend to give higher values of t_o as observed.

The calculated temperature rise of 3.5°C compared with the measured "steady-state" value of 1.0°C needs some explanation. Of course, the capacitance and contact resistance of the thermistor would tend to give rise to the lower measured value. But more important is the fact that the predicted value is for the granular carbon continuum which is linked to the brass dome through a contact resistance. The temperature drop across that resistance can be calculated by multiplying the temperature rise above ambient (θ) by the ratio of the contact resistance ($1/h_c$) to the total resistance ($1/h_{tot}$);

$$\Delta T_{\text{continuum to thermistor}} = \frac{\theta(1/h_c)}{1/h_{tot}} = 2.4^\circ\text{C}.$$

Therefore, $\Delta T_{\text{thermistor above ambient}} = 3.5^\circ\text{C} - 2.4^\circ\text{C} = 1.1^\circ\text{C}$; which is in remarkably good agreement with the measured value of 1.0°C . The other measured values, at the end of the early transient (namely, 0.33°C , 1.56°C , and 1.61°C), scale linearly with the input power; hence, the agreement with analysis remains good for all the results given in Fig. 10.

Consider briefly a transmitter made of invar. For invar the k_d value is 18 times smaller than that of aluminum. Consequently,

$$1/h_{tot} = 1/36.6 + 1/300;$$

hence

$$h_{tot} = 32.6 \text{ W}/(\text{m}^2 \cdot ^\circ\text{C})$$

and $N_{Bi} = 0.4$. From Fig. 6 we see that the temperature rise would be 1.74 times that under corresponding conditions in the T1 transmitter. From Fig. 9 the value of t_o would be 30 percent longer. This is in qualitative agreement with the observations of Fischer and Gaudet.²

Turning now to the displacement we first calculate the extension of the slant height of the aluminum diaphragm using (43). Taking $\nu = 1/3$ and $\alpha_t = 23.4 \times 10^{-6} \text{ } ^\circ\text{C}^{-1}$ we obtain for a temperature rise of 1°C

$$u = -0.029 \text{ } \mu\text{m}.$$

The minus sign indicates that the diaphragm grows toward the dome electrode. The expansion of the dome electrode is obtained from (37) using $\alpha_t = 16.2 \times 10^{-6} \text{ } ^\circ\text{C}^{-1}$ for brass. For $\theta = 1^\circ\text{C}$, $\Delta r = 0.04 \text{ } \mu\text{m}$. The minimum displacement, given by (45), becomes $0.0064 \text{ } \mu\text{m}$, while the maximum displacement given by (46) becomes

$$\Delta h_{\text{max}} = \frac{\alpha_t \theta a}{\tan \alpha} - \frac{u}{\sin \alpha} = 0.180 + 0.134 = 0.32 \text{ } \mu\text{m}.$$

The upper limit which assumes a perfectly rigid dome electrode compares reasonably well with the measured value of $0.18 \text{ } \mu\text{m}$ from Fig. 10b. Notice that the top of the dome electrode moves an additional $0.04 \text{ } \mu\text{m}$.

The most significant factor arising out of this rather crude model for displacements is that the thermal packing appears to be more sensitive to the thermal expansion coefficient for the dome electrode than any other part. Hence, a simple and inexpensive modification of the T1 transmitter would have been to change only the dome electrode to invar. Although the above analysis does not strictly apply to the modified transmitter design of Huffstutler,¹ the same conclusion with regards to an invar dome seems appropriate.

The thermal expansion of the carbon produces an additional packing effect. The change in volume caused by the heating could be calculated by using the expansion coefficient value⁵ of $10.4 \times 10^{-6} \text{ } ^\circ\text{C}^{-1}$ and the local temperature as given in Fig. 7. An estimate of such a calculation yields a dome displacement equivalent to $0.05 \text{ } \mu\text{m}$ in the direction opposite the displacements mentioned above for the conditions of Fig. 10b.

V. CONCLUSIONS

The resistance change of the T1 transmitter resulting from the joulean heating can be associated with the thermal expansion of the dome electrode and the aluminum diaphragm. The agreement of the model presented here with the measurements of Sandahl and Prettyman attests to its validity for the early time transients. The displacements which produce thermal packing are a stronger function of the

thermal expansion coefficient of the dome electrode than any other part. A simple modification would be to make this part of invar in the T1 or any similar transmitter. The model also demonstrates that the displacements associated with the temperature rise of the dome electrode are affected less by changing the thermal parameters of the system than by reducing the thermal expansion coefficient in going from aluminum and brass to invar. The thermal contact resistance between the granular carbon and the dome electrode reduces the temperature rise significantly.

VI. ACKNOWLEDGMENT

The author wishes to acknowledge the stimulating discussions with R. J. Port and the suggestion by R. J. Grosh of the existence of a contact resistance.

APPENDIX A

Localized Heating in the Carbon Granules

Because of the asperities of carbon granules and of the "bunching up" of the current flow at the contact areas, the importance of localized heating should be checked. It can be assumed that the localized effects are virtually all diffused at the values of time for which the Fourier modulus $\kappa t_0/D^2$ is approximately unity. Then on setting the characteristic dimension of the granule, D equal to 0.2 mm, and the thermal diffusivity, κ , of solid carbon equal to 0.2×10^{-4} m² per second, the value of the time constant, t_0 , becomes approximately

$$t_0 = D^2/\kappa = \frac{(0.2)^2 \times 10^{-6}}{0.28 \times 10^{-4}} = 1.4 \text{ msec.}$$

We see that the thermal time constant for the solid carbon granules is at least three orders of magnitude less than the thermal time constant of the thermal effects being observed. Consequently, any localized heating is rapidly diffused and the granular carbon can be treated as a continuum.

APPENDIX B

Transient Temperature Response of the Carbon Chamber

Consider the transient portion of the heat conduction problem specified by (24) through (27) and repeated below for convenience.

$$\partial\vartheta/\partial\tau = \partial^2\vartheta/\partial\eta^2 \quad (50)$$

$$\vartheta(\eta, 0) = F/(1 - F) \left[\frac{1}{1 - (1 - F)\eta} \right] - \varphi(\eta) \quad (51)$$

$$\vartheta(0, \tau) = 0 \quad (52)$$

$$\partial\vartheta/\partial\eta(1, \tau) + \frac{(1 - F)}{F} (N_{Bi} + 1)\vartheta(1, \tau) = 0. \quad (53)$$

Assuming a separable solution of the form

$$\vartheta(\eta, \tau) = X(\eta)T(\tau) \quad (54)$$

so that

$$X = A \sin \lambda\eta + B \cos \lambda\eta \quad (55)$$

$$T = Ce^{-\lambda^2\tau}. \quad (56)$$

But (52) requires that $B = 0$ and (53) specifies that

$$\lambda A \cos \lambda + c_1 A \sin \lambda = 0$$

or,

$$\lambda \cot \lambda = -c_1 \quad (57)$$

where

$$c_1 = \frac{(1 - F)}{F} (N_{Bi} + 1). \quad (58)$$

To satisfy the nonhomogeneous initial condition we set

$$\vartheta(\eta, 0) = \sum_{n=1}^{\infty} A_n X_n, \quad (59)$$

where $X_n = \sin \lambda_n \eta$ and λ_n is the n th positive root of (57). Multiplying both sides of (59) by X_m , integrating, and using the orthogonality condition we have

$$A_n = \frac{\int_0^1 X_n(\eta) \vartheta(\eta, 0) d\eta}{\int_0^1 X_n^2 d\eta}. \quad (60)$$

Evaluating the integral in the denominator where the boundary conditions have been used we have

$$\int_0^1 X_n^2 d\eta = \frac{\lambda_n^2 + c_1^2 + c_1}{2(\lambda_n^2 + c_1^2)}. \quad (61)$$

The transient part of the solution can thus be written as

$$\vartheta(\eta, \tau) = \sum_{n=1}^{\infty} \frac{2(\lambda_n^2 + c_1^2)}{\lambda_n^2 + c_1^2 + c_1} \exp(-\lambda_n^2 \tau) \sin \lambda_n \eta \int_0^1 \vartheta(\eta, 0) \sin \lambda_n \eta d\eta. \quad (62)$$

To evaluate the integral in (62) we first notice that (51) can be written as

$$\vartheta(\eta, 0) = c_0 - c_2 \eta + \frac{c_3}{1 - c_4 \eta}$$

so that

$$\begin{aligned} \int_0^1 \vartheta(\eta, 0) \sin \lambda_n \eta d\eta &= c_0/\lambda_n [1 - \cos \lambda_n] - c_2/\lambda_n^2 [\sin \lambda_n - \lambda_n \cos \lambda_n] \\ &+ c_3 \int_0^{\lambda_n} \frac{\sin \xi d\xi}{\lambda_n - c_4 \xi}. \end{aligned} \quad (63)$$

The last term which can be expressed in various forms is the one which causes the series to converge very slowly.

REFERENCES

1. Huffstutler, M. C., Jr., and Kerns, B. T., unpublished work.
2. Fischer, C. A. and Gaudet, G. G., unpublished work.
3. Timoshenko, S. and Goodier, J. N., *Theory of Elasticity*, New York: McGraw-Hill, 1951, p. 407.
4. Fritsch, C. A. and P. E. Prettyman, "Measurements of the Thermal Conductivity of Granular Carbon and the Thermal Contact Resistance at the Container Walls," Proc. 7th Conf. Thermal Conductivity, Nat. Bureau of Standards, Gaithersburg, Maryland, November 13-15, 1967.
5. Booth, T. C., unpublished work.